Molecular Cell
Article

Noncooperative Interactions between Transcription Factors and Clustered DNA Binding Sites Enable Graded Transcriptional Responses to Environmental Inputs

Luca Giorgetti,[1] Trevor Siggers,[2] Guido Tiana,[3,4] Greta Caprara,[1] Samuele Notarbartolo,[1] Teresa Corona,[6] Manolis Pasparakis,[4] Paolo Milani,[4,5] Martha L. Bulyk,[2,7,8] and Gioacchino Natoli[1,*]
[1]Department of Experimental Oncology, European Institute of Oncology, IFOM-IEO Campus, 20139 Milan, Italy
[2]Division of Genetics, Department of Medicine, Brigham and Women's Hospital and Harvard Medical School, Boston, MA 02115, USA
[3]INFN
[4]Dipartimento di Fisica
[5]CIMAINA
Universita' di Milano, 20133 Milan, Italy
[6]Institute for Genetics, University of Cologne, 50674 Cologne, Germany
[7]Department of Pathology, Brigham and Women's Hospital and Harvard Medical School, Boston, MA 02115, USA
[8]Harvard-MIT Division of Health Sciences and Technology, Harvard Medical School, Boston, MA 02115, USA
*Correspondence: gioacchino.natoli@ifom-ieo-campus.it
DOI 10.1016/j.molcel.2010.01.016

SUMMARY

A paradigm in transcriptional regulation is that graded increases in transcription factor (TF) concentration are translated into on/off transcriptional responses by cooperative TF binding to adjacent sites. Digital transcriptional responses underlie the definition of anatomical boundaries during development. Here we show that NF-κB, a TF controlling inflammation and immunity, is conversely an analog transcriptional regulator that uses clustered binding sites noncooperatively. We observed that increasing concentrations of NF-κB are translated into gradual increments in gene transcription. We provide a thermodynamic interpretation of the experimental observations by combining quantitative measurements and a minimal physical model of an NF-κB-dependent promoter. We demonstrate that NF-κB binds independently to adjacent sites to promote additive RNA Pol II recruitment and graded transcriptional outputs. These findings reveal an alternative mode of operation of clustered TF binding sites, which might function in biological conditions where the transcriptional output is proportional to the strength of an environmental input.

INTRODUCTION

A commonly held view is that genes exist in only two alternative functional states, namely active or inactive, with enhancers controlling the probability but not the rate of transcription (Walters et al., 1995). In this view, a graded increase in transcription factor (TF) concentration is translated into a digital (on/off) transcriptional response, enabled by cooperative TF binding to adjacent sites (Segal et al., 2008) (Figure 1). This paradigm applies well to TFs operating in developmental processes, notably embryonic segmentation, which require the definition of sharp anatomical borders. A classic example is the morphogen model of Bicoid (Bcd) action in *Drosophila* embryogenesis. Cooperative binding of Bcd to adjacent DNA sites represents the molecular basis by which a gradual protein gradient of Bcd along the anterior-posterior embryonic axis is converted into a sharp on/off pattern of expression of Bcd target genes (Burz et al., 1998; Gregor et al., 2007). Nonetheless, clusters of adjacent binding sites for a given TF ("homotypic clusters"), as well as heterotypic clusters containing binding sites for multiple TFs, are a widespread genomic feature of higher eukaryotes (Arnone and Davidson, 1997; Berman et al., 2002; Lifanov et al., 2003; Markstein et al., 2002), and it is not intuitively obvious that on/off switches arising from the cooperative usage of such clustered sites may be compatible with biological responses other than those requiring the definition of well-demarcated gene expression domains.

Responses to environmental perturbations are conditions where the degree of gene activation is commensurate with the strength of the inducing stimulus. A well-known example is the inflammatory response induced by microbes, in which the intensity of the response is proportional to the microbial load. As another example, the p53 response to X or UV rays increases in proportion to the intensity of irradiation (Lahav et al., 2004). In principle this linear input/output (i/o) relationship may be achieved in at least three different ways: (1) by devising transcriptional regulatory circuits allowing transcription to be tuned to the intensity of the stimulus at the level of individual cells, (2) by increasing the fraction of cells in a population that are digitally activated in response to increasing doses of stimulus (Podtschaske et al., 2007), or (3) by increasing the number of consecutive pulses of gene activation occurring in individual cells in response to increasing doses of the stimulus (Lahav et al., 2004). The first of these models requires that the system be

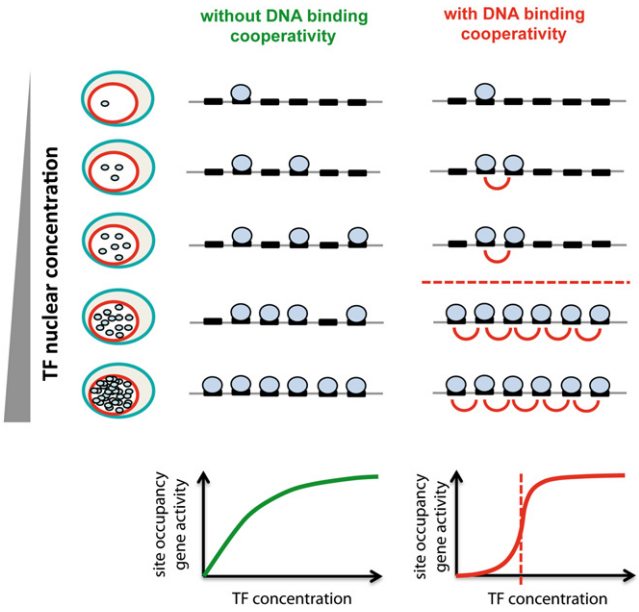

Figure 1. DNA Binding Cooperativity Generates Sharp Transcriptional Boundaries

If a TF binds to a cluster of DNA binding sites in a noncooperative manner, a gradual increase in TF concentration generates a gradual increase in the average occupancy of the cluster. Conversely, if TF binding to adjacent sites is cooperative, a gradual increase in TF concentration generates a "digital" on/off response as the concentration sweeps a threshold value (dashed line). The higher binding cooperativity, the steeper the transition between the "off" and the "on" states.

able to accurately sense, transduce, and exploit at the transcriptional level the regulatory information provided by a broad range of concentrations of the stimulus. This highly intuitive and rational operational mode, for which no unequivocal evidence has been provided, implies a continuous spectrum of outputs in response to a continuous spectrum of inputs. Cellular responses to cytokines, whose concentration in body fluids varies across orders of magnitude in response to stimulation, should provide an ideal experimental setting to challenge this model.

NF-κB/Rel is a family of dimeric TFs conserved from flies to humans that controls transcription of hundreds of genes implicated in inflammatory and immune responses (Hayden and Ghosh, 2008). The most common NF-κB dimer in mammalian cells is p50/p65, which binds to decameric DNA sequences (Natoli et al., 2005). p50/p65 and most other NF-κB dimers are sequestered in the cytoplasm of unstimulated cells by association with inhibitory proteins, the IκBs. In order to allow nuclear translocation of NF-κB in response to stimulation, the IκBs are phosphorylated and degraded. IκBα (encoded by the *NFKBIA* gene) is both the most rapidly degraded IκB protein and the most rapidly resynthesized one, by virtue of a negative feedback based on NF-κB binding and activation of the *NFKBIA* promoter (Hoffmann et al., 2002).

The *D. melanogaster* Rel family TF Dorsal cooperates with itself and other TFs (like Twist) to establish sharp patterns of expression of its target genes during embryo development (Ip et al., 1992; Stathopoulos and Levine, 2002), indicating that selected NF-κB/Rel TFs can direct digital patterns of developmental gene expression using cooperative interactions (Gonzalez-Crespo and Levine, 1993; Roth et al., 1989). Importantly, when Dorsal-deficient embryos were reconstituted with Dif, a Rel family protein involved in the immune response, Dorsal target genes were activated, but the spatial precision arising from cooperative binding of Dorsal to DNA was lost (Stein et al., 1998). Thus, even closely related TFs binding to the same or similar DNA motifs but operating in different biological contexts exhibit different properties regarding cooperativity in binding.

Here we report that, in contrast with the classical models of on/off developmental gene regulation, clusters of NF-κB binding sites are organized to generate transcriptional outputs whose intensity varies with that of the stimulus. The interpretation of the response curves in terms of a thermodynamic model adapted to the analysis of TF-DNA interactions indicates that the graded response is a consequence of noncooperative binding of NF-κB to clustered sites in *cis*-regulatory elements (CREs). We propose that such an analog type of regulation may best fit the requirements of most TFs controlling responses to environmental stimuli.

RESULTS

Genome-wide Analysis of Clusters of Conserved NF-κB Binding Sites

We began by investigating the presence of evolutionarily conserved clusters of NF-κB binding sites ("κB sites") in the proximal promoter regions (−1000 bp to +200 bp relative to transcription start sites, TSSs) of 24,398 human RefSeq genes. κB sites were predicted using an available NF-κB position weight matrix (PWM) (Grilli et al., 1993). Phylogenetic conservation has been shown to provide a useful filter to enrich for functional binding sites identified in genome scans (Gumucio, 1991), although a sizeable fraction of active regulatory elements lacks detectable sequence constraints (Birney et al., 2007; Ponting, 2008). In our initial genome scan we used a simple, relatively strict phylogenetic filter, requiring that for each κB site identified in the human genome a κB site was also found in the aligned sequence of more than half of the 11 mammalian genomes examined.

We identified 24 clusters comprising three or more conserved κB sites upstream of 23 genes (see Table 1). Comparing this list of genes to a curated list of NF-κB targets (from http://nfkb.org/) we found that it was significantly enriched for known NF-κB target genes ($p = 1.6 \times 10^{-10}$, Fisher's exact test). Of note, this short list contained two known negative regulators of NF-κB signaling: *NFKBIA*, encoding IκBα, was one of the two top-scoring genes in the genome with five deeply conserved κB sites (see Figure 2A); and *TNFAIP3*, encoding the negative regulator A20 (Werner et al., 2008), had three κB sites in its promoter. Also identified were two members of the Rel family itself: *REL*, encoding the c-Rel protein, had three κB sites; and two different isoforms of *NFKB2*, encoding p105/p50, had clusters of three κB sites.

Table 1. Genome-wide Analysis of Clusters of Conserved κB Sites

Gene Name	RefGene ID	Number of κB Sites, Conserved in Six Genomes	Number of κB Sites, Conserved in Four Genomes	Number of κB Sites, Total	Inter-κB Distances	Known NF-κB Targets
NFKBIA	NM_020529	5	5	6	29 97 98 62 67	*
PTCHD1	NM_173495	5	5	5	97 267 54 23	
RCOR2	NM_173587	4	4	5	41 34 138 28	
CAMTA1	NM_015215	4	4	4	31 59 29	
UTP18	NM_016001	4	4	4	281 131 387	
CACNA1G	NM_198397	3	5	6	109 334 189 160 43	
PSME2 | RNF31	NM_002818 | NM_017999	3	4	6	52 104 137 93 72	*
SPIB	NM_003121	3	4	6	256 47 78 260 26	
CCL20	NM_004591	3	4	5	15 261 32 17	*
IL28B	NM_172139	3	4	4	230 62 15	
NFKB2 (c1)	NM_002502	3	3	5	64 54 136 155	*
NFKB2 (c2)	NM_001077493	3	3	4	59 224 29	*
TNFAIP3	NM_006290	3	3	4	22 185 12	*
BCL2L1	NM_001191	3	3	3	270 172	*
GRIN2B	NM_000834	3	3	3	350 128	
GRIN2D	NM_000836	3	3	3	327 22	
HES1	NM_005524	3	3	3	25 76	
ITGA5	NM_002205	3	3	3	35 285	
ITPR1	NM_002222	3	3	3	133 229	
REL	NM_002908	3	3	3	300 286	*
RHOG	NM_001665	3	3	3	62 200	
TRIB1	NM_025195	3	3	3	62 200	
TSSK3	NM_052841	3	3	3	19 323	
WNT1	NM_005430	3	3	3	185 212	
CSF1	NM_0172210	1	3	4	60 19 315	*
NFKB1	NM_003998	2	3	3	192 92	*
IRF1	NM_002198	1	2	4	241 368 231	*

Listed are the 24 κB site clusters (three or more κB sites, within 400 bp of each other, conserved in at least six aligned mammalian genomes) identified in the promoters of 24,398 human RefSeq genes (see the Experimental Procedures). Clusters for *NFKB1*, *CSF1*, and *IRF1* are also listed. Columns 1 and 2 list the gene names and RefSeq IDs for genes associated with each cluster. Columns 3–5 list the number of κB sites within each cluster at decreasing conservation threshold for κB sites: at least six genomes, at least four genomes, and no conservation, respectively. Column 6 lists the intersite distances for all nonconserved κB sites within each cluster.

To determine if all κB sites within these promoters were conserved, we repeated the genome scan using relaxed conservation constraints, requiring either site conservation in at least four mammalian genomes or no conservation at all (Table 1, columns 4 and 5, respectively). About half (12/23) of the genes have an additional κB site that did not reach our initial conservation threshold. Table 1 includes three additional genes, *NFKB1*, *CSF1*, and *IRF1*, which were not identified as having clusters at our most rigid conservation threshold, but do have clusters at our intermediate conservation requirement, and which are known to be regulated by NF-κB (Hoffmann et al., 2003). The presence of multiple, conserved κB sites within the promoters of genes encoding NF-κB family members (*NFKB1*, *NFKB2*, *REL*) and negative regulators of NF-κB activity (*NFKBIA*, *TNFAIP3*) suggests a specific regulatory role for promoter-proximal κB site clusters in the regulatory network controlling NF-κB function.

A Gradual Input-Output Relationship in the NF-κB Transcriptional Response

To investigate how clustered κB sites are used, we measured the i/o relationship between the nuclear concentration of NF-κB and the transcriptional activity of its target genes. To this aim, we first sought to generate a smooth gradient of nuclear NF-κB that could be used as an input probe. We exposed human HCT116 cells, a colonic epithelial cell line, to increasing concentrations of the inflammatory cytokine tumor necrosis factor alpha (TNF-α) in order to induce NF-κB release from the IκBs and to promote its nuclear accumulation. The maximal nuclear concentration of p65, which in these cells is achieved 30 min after the beginning of stimulation (data not shown and Figure 3A), is monotonically dependent on the TNF-α dose (see Figures S1A and S1B available online): the higher the TNF-α dose, the higher the maximal nuclear NF-κB occupancy. Importantly, the entire cell population responded uniformly to increasing TNF-α concentrations

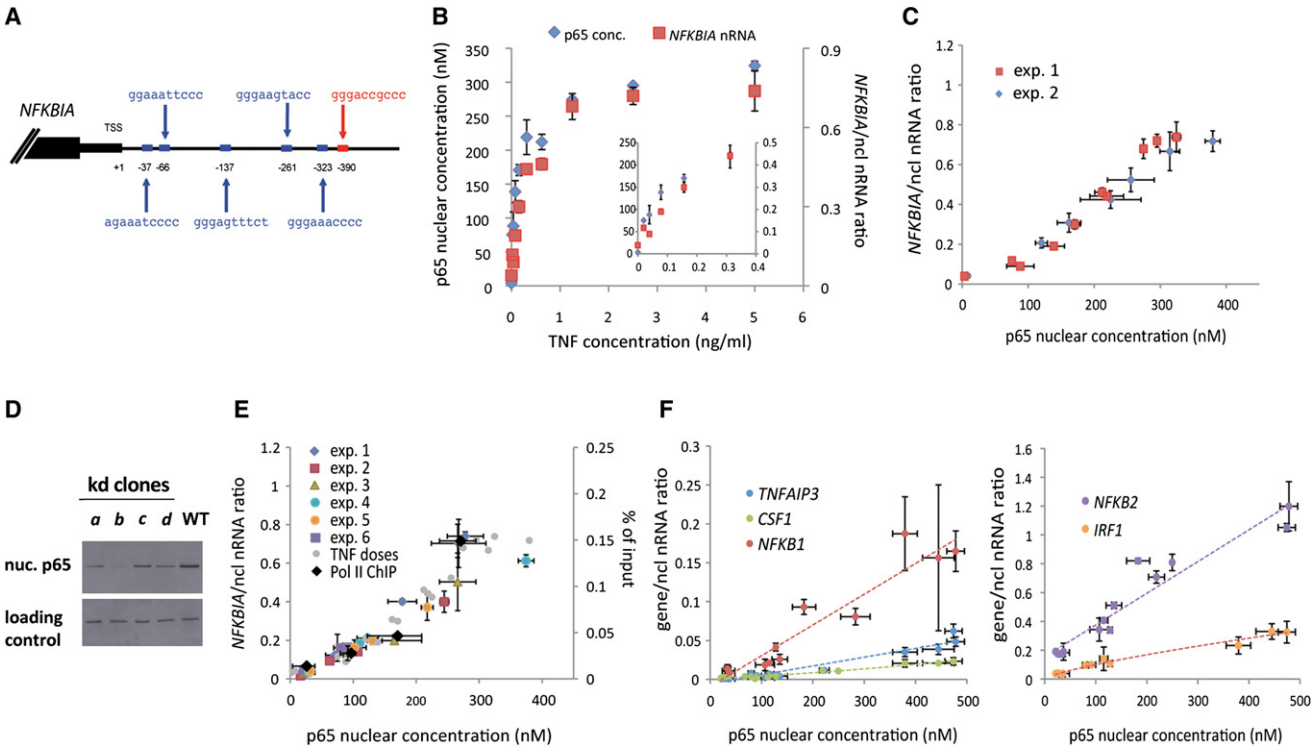

Figure 2. The Analog Nature of the Inflammatory Transcriptional Response

(A) Schematics of the human *NFKBIA* promoter region. The five conserved κB sites, along with their sequences, are shown in blue, the human-specific κB site in red.

(B) Induction of nuclear p65 and *NFKBIA* nascent transcripts (nRNA) in WT HCT116 cells stimulated with increasing doses of TNF-α (20 min). The average p65 nuclear concentration is expressed in nM (mean ± SD in ELISA duplicate assays from a single experiment). The *NFKBIA* nRNAs are normalized to the nascent transcripts of nucleolin (*ncl*) (mean ± Q-PCR error propagated from SD of technical replicates of a representative experiment). (Inset) Magnification of the low TNF-α concentration regime.

(C) The amount of *NFKBIA* nascent transcripts versus nuclear p65 concentration in cells treated with increasing doses of TNF-α. Data collected in two independent experiments (blue and red markers) are plotted.

(D) p65 was downregulated by RNAi to differential residual amounts in clonal HCT116 cell lines. Nuclear p65 in different clones was detected by western blot (20 min stimulation with 10 ng/ml TNF-α).

(E) *NFKBIA* nascent transcripts versus nuclear p65 concentration in p65 knockdown clonal cell lines stimulated with 10 ng/ml TNF-α for 20 min (different experimental points represent different clonal cell lines). Data were collected in six independent experiments and labeled with different colors. Gray markers, data obtained in WT cells stimulated with increasing doses TNF-α, see (C). Black markers, anti-Pol II ChIP in p65 knockdown clones treated with TNF-α for 20 min. Immunoprecipitated DNA was amplified by Q-PCR with the same primers used to amplify *NFKBIA* nascent transcripts. DNA recovery was expressed as percent of input (mean ± Q-PCR error propagated from SD of technical replicates of a single representative experiment).

(F) The nascent transcripts of a panel of NF-κB target genes are plotted versus p65 nuclear concentration in p65 knockdown clonal cell lines stimulated with 10 ng/ml TNF-α for 20 min (mean ± Q-PCR error propagated from SD of technical replicates of a single representative experiment). Dashed lines, linear interpolations to the data.

(Figure S1B), indicating that the average value of nuclear concentration of NF-κB is representative of the population (Figure S1C). The average nuclear concentration is almost linearly dependent on the extracellular TNF-α concentration in the low TNF regime and saturates at approximately 300 nM at high TNF-α doses (Figure S1C). Thus, the relationship between TNF-α concentration and nuclear entry of NF-κB is gradual, with no evidence of cooperative effects in signal transduction. Importantly, the range of TNF-α concentrations used here extensively overlaps the concentrations found in vivo in various conditions, e.g., from 0.05 to 0.7 ng/ml in acute phase reactions (Maury, 1989), and up to 1–2 ng/ml in the sinovial fluid of patients with rheumatoid arthritis (Tetta et al., 1990).

We used this monotonic gradient of nuclear NF-κB concentration to probe the transcriptional activity of IκBα, which we considered as a model NF-κB target gene. We posit that, IκBα being the main negative feedback regulator of the NF-κB pathway, its regulation should be entirely controlled by NF-κB, an assumption supported by experimental data (Hoffmann et al., 2003). Therefore, the NF-κB-IκBα relationship is the simplest (and the most tractable) in transcriptional control: a single TF being the primary or only determinant of the activation of a target gene.

To measure the *NFKBIA* transcription rate in real time, we quantified the nascent, chromatin-associated transcripts of *NFKBIA* in parallel with the NF-κB nuclear concentration after

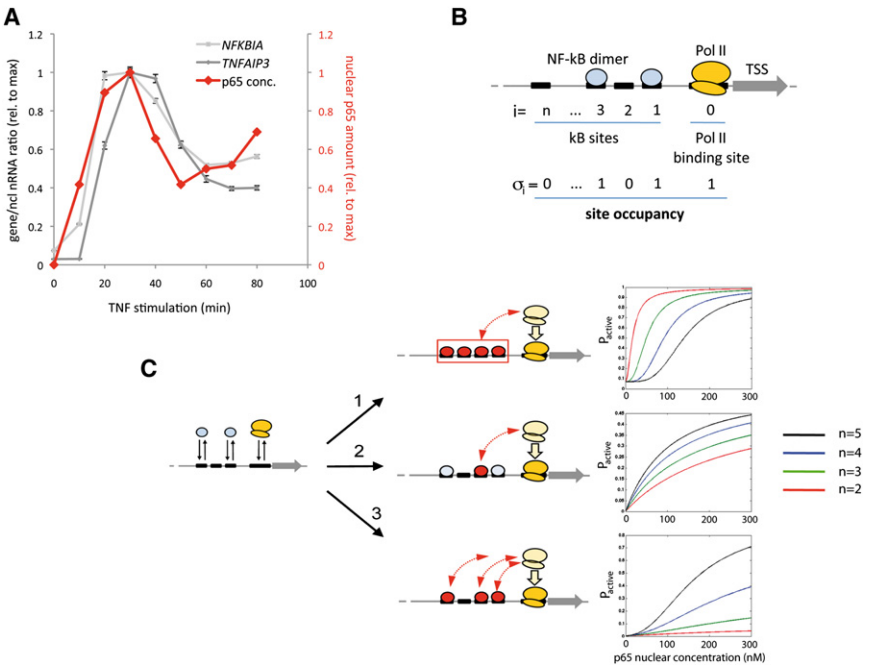

Figure 3. An Equilibrium Statistical Mechanics Model of Promoter Operation

(A) NF-κB-dependent transcription of inflammatory genes occurs at kinetic equilibrium. Time course of NF-κB nuclear occupancy (red line) and transcription of *NFKBIA* and *TNFAIP3* (gray lines) during stimulation of HCT 116 cells with 10 ng/ml TNF-α. Data were renormalized to the maxima at 30 min, and errors in Q-PCR quantification were propagated accordingly.

(B) Schematics of the model of promoter operation, wherein *n* κB sites are arrayed in a 1D arrangement along with a Pol II binding site. The model is formally equivalent to a finite 1D Ising model with *n + 1* spin variables.

(C) Model variants concerning the usage of NF-κB binding sites in a cluster. NF-κB exchanges at equilibrium with each site on DNA, and Pol II exchanges at equilibrium with the core promoter site, independently from the rules concerning their mutual interaction. Once bound to the cluster, TFs interact with Pol II via an effective attractive interaction energy, either in an all-or-none fashion (1), singularly (2), or additively (3). Each hypothesis concerning site usage leads to different outputs regarding the transcriptional activation of a gene with a certain number of sites, as a function of the nuclear NF-κB concentration.

20 min of TNF-α treatment (Figure 2B). Briefly, from isolated nuclei we extracted chromatin and its physically associated nascent transcripts, and we also measured the average functional (DNA binding-competent) p65/p50 concentrations. *NFKBIA* transcription, averaged over the cell population, gradually increased with increasing NF-κB nuclear concentrations, with no abrupt transition from the inactive to the active state (Figure 2C). The rationale for performing the experiments after 20 min of TNF-α treatment was to avoid the appearance of newly synthesized IκBα.

To validate the assumption that nuclear NF-κB concentration is the only determinant of the observed trend of *NFKBIA* transcriptional activity, we produced stable, clonal HCT116 cell lines in which p65 is downregulated by RNA interference, each cell line expressing a different residual amount of p65 (Figure 2D). In these cell lines, the p65 nuclear concentration after 20 min of TNF-α treatment spans from a minimum of 10 nM to a maximum of approximately 400 nM, providing a broad range of TF concentration to be used in downstream gene regulatory circuits, in a context where the external stimulus (TNF-α), and therefore the level of activation of collateral signaling pathways and TFs, is kept constant. We simultaneously stimulated these cell lines with the same concentration of TNF-α for 20 min and quantified the p65 nuclear amount and the *NFKBIA* nascent transcripts. We observed gradually increasing transcription as a function of gradually increasing nuclear concentration of NF-κB (Figure 2E). To confirm that nascent transcripts faithfully reflected the degree of gene activation, we measured the RNA polymerase II (Pol II) occupancy of *NFKBIA* by chromatin immunoprecipitation (ChIP), which was consistent with a gradual relationship between NF-κB nuclear concentrations and gene activity (Figure 2E). Of note, the induction profile measured in knockdown clones could be precisely superimposed to the one obtained in wild-type cells stimulated with increasing doses of TNF-α, which demonstrated that p65 nuclear concentration is the main determinant of the level of *NFKBIA* transcriptional activity, and that the transcriptional activity of *NFKBIA* is precisely tuned to the concentration of nuclear NF-κB.

We found that this gradual transcriptional response is not an exclusive feature of *NFKBIA* but rather is common to all the other NF-κB-regulated genes we tested (*TNFAIP3*, *NFKB1*, *NFKB2*, *IRF1*, *CSF1*) (Figure 2F). This is an important observation, since at least some of these genes are not exclusively NF-κB targets but rather are coregulated by additional TFs that may contribute to tuning the transcriptional output to additional environmental or internal cues. Our data show that, irrespective of the exclusive or nonexclusive role of NF-κB in the control of target gene expression, the information related to the dynamic range of input is extensively and precisely exploited by the downstream gene regulatory circuits. Notably, given a specific nuclear concentration of p65, *NFKBIA* transcriptional output was highly reproducible by both experimental approaches used to tune nuclear p65 levels (Figure 2E). Thus, the cellular response to TNF-α is highly accurate and sensitive at a wide range of levels, from the detection of the concentration of the primary stimulus to the generation of a transcriptional response that is proportional to the nuclear levels of NF-κB.

These data show that the inflammatory response has an entirely analog nature, wherein a graded increase in TNF concentration leads to a graded increase in nuclear NF-κB concentration and an associated increase in transcription of target genes. The analog nature of the NF-κB i/o transcriptional relationship is contrary to the one reported to be characteristic of developmental TFs (Gregor et al., 2007). Moreover, it implies

that the regulatory capacity of the NF-κB response is higher than that of binary switches, which allow only two states (on/off) of gene activity.

A Model of NF-κB-Dependent Promoter Operation Based on Equilibrium Statistical Mechanics

We next asked how clusters of κB sites orchestrate the observed analog response. Specifically, given that cooperative TF binding to adjacent sites underlies digital transcriptional responses in development, we asked if the behavior we found might conversely reflect (and require) *noncooperative* binding of NF-κB to clustered sites. And if this were the case, what are the mechanisms regulating Pol II activity in response to noncooperative binding to the clusters?

A precise understanding of how κB sites operate biochemically requires resolving binding site occupancy at single-site, single-cell resolution, which is currently not possible given the very short distance between adjacent sites (Table 1) and the limited resolution of ChIP. To overcome these limitations and to address the questions above, we developed a minimal physical model of a multisite promoter. Our physical model is based on the thermodynamics of NF-κB binding and its interaction with RNA Pol II. The model is defined by four numerical constants: the number of κB sites, and the binding free energies of NF-κB to its DNA binding sites, to the RNA polymerase and between NF-κB molecules bound within the cluster (i.e., binding cooperativity).

The model relies on equilibrium statistical mechanics, motivated by the observation that the NF-κB response mechanism operates at equilibrium. This is supported by the observation (Figure 3A) that the transcriptional activity of NF-κB target genes is synchronous to the variation of NF-κB concentration, which implies that the promoter is able to rapidly gauge changes in nuclear NF-κB concentration. Thus all binding and unbinding events at the promoter, as well as Pol II transition from the initiating to the elongating state, occur on a much shorter timescale as compared to the variation in NF-κB nuclear levels; these results are supported by previous experimental observations (Bosisio et al., 2006; Darzacq et al., 2007). When the nuclear NF-κB concentration varies, processes at the promoter equilibrate kinetically, with changes in NF-κB concentration being rapidly translated into changes in gene transcription. These observations provide direct evidence for equilibrium conditions in NF-κB-dependent transcription and therefore support the use of an equilibrium model to interpret experimental data.

We thus assume that NF-κB exchanges at equilibrium with *n*-specific sites in the promoter region. We further assume that Pol II binding to the core promoter occurs at equilibrium, and that bound NF-κB molecules interact with Pol II via an effective attractive interaction (Figures 3B and 3C), independently of the number of intermediate adapters. When provided with the nuclear concentration of NF-κB, the model returns the average transcriptional activity of the target gene; this has a direct experimental counterpart in the induction curves shown in Figure 2. The model is well suited to describe our experimental setup, wherein the cell population provides the statistical ensemble of replicas of the system. Moreover, it can be solved analytically being formally equivalent to a one-dimensional (1D) finite Ising model coupled to an external field. This latter (Huang, 1987) was originally developed as a simplified model of ferromagnetic materials, which contain ordered arrangements (lattices) of atoms possessing a magnetic moment (spin), and was later adapted to diverse biophysical systems including DNA condensation (Palmeri et al., 2008), nucleosome positioning (Ishii, 2000), and protein folding (Munoz, 2001). Here we show that in its 1D formulation, it is formally equivalent to the problem of equilibrium binding of a TF to a cluster of specific binding sites in a promoter sequence, the cluster of binding sites corresponding to an ordered arrangement (a lattice) of atoms. In the formal equivalence we derive (Supplemental Information), the average Pol II occupancy of the core promoter, which we assume to be proportional to the probability of activating transcription (Darzacq et al., 2007), is obtained by adapting the known solutions of the 1D Ising model to calculate the average value of the occupancy state of the Pol II binding site. Similarly, the average NF-κB occupancy on the cluster is obtained by calculating the average occupation state of the promoter sites (which is equivalent to the average "magnetization" in the classical Ising model of ferromagnets). As compared to other existing approaches (Bintu et al., 2005; Segal et al., 2008), our model has several advantages. First, it returns explicit expressions for the observables of interest, with no need for computer simulations even in the presence of binding cooperativity. Second, once the number of sites and the TF binding constant are fixed (see below), it contains only four free parameters, all having a clear biological significance. Third, our approach allows calculating straightforwardly several important properties of the system, notably the fluctuations in Pol II occupancy (which are related to the intrinsic noise in transcription, and allow taking into account random errors in a rigorous way when analyzing experimental data; see the Supplemental Information).

We formulated three equally plausible a priori hypotheses about the usage of κB sites in a cluster, each hypothesis returning a qualitatively and quantitatively different output (Figure 3C). First, we hypothesized that all binding sites in a cluster need to be bound simultaneously to recruit Pol II to the promoter. This would result in *limiting the transcriptional activation of genes with many sites*, by requiring TF concentrations high enough to saturate binding to the cluster (Figure 3C, scheme 1). Although counterintuitive at first, this mode of operation might ensure that, for instance, IκBα is not induced before a given nuclear concentration of NF-κB is reached, thus preventing a premature shutoff of the response. A second possibility is that one NF-κB molecule, bound to any site within the cluster, is sufficient to recruit Pol II. Upon this assumption, the role of the cluster would be to increase the *probability* of TF binding to the promoter. Genes whose regulatory regions have a high number of sites would be induced at lower TF concentrations as compared to genes with fewer binding sites (Figure 3C, scheme 2). A third possibility is that all DNA-bound NF-κB molecules attract Pol II independently, with each NF-κB molecule contributing to Pol II recruitment in an additive manner. This would result in an *expanded dynamic range* for genes with a high number of binding sites, which would possess a higher sensitivity to changes in NF-κB nuclear concentration and higher maximal transcriptional activities as compared to genes with fewer sites (Figure 3C,

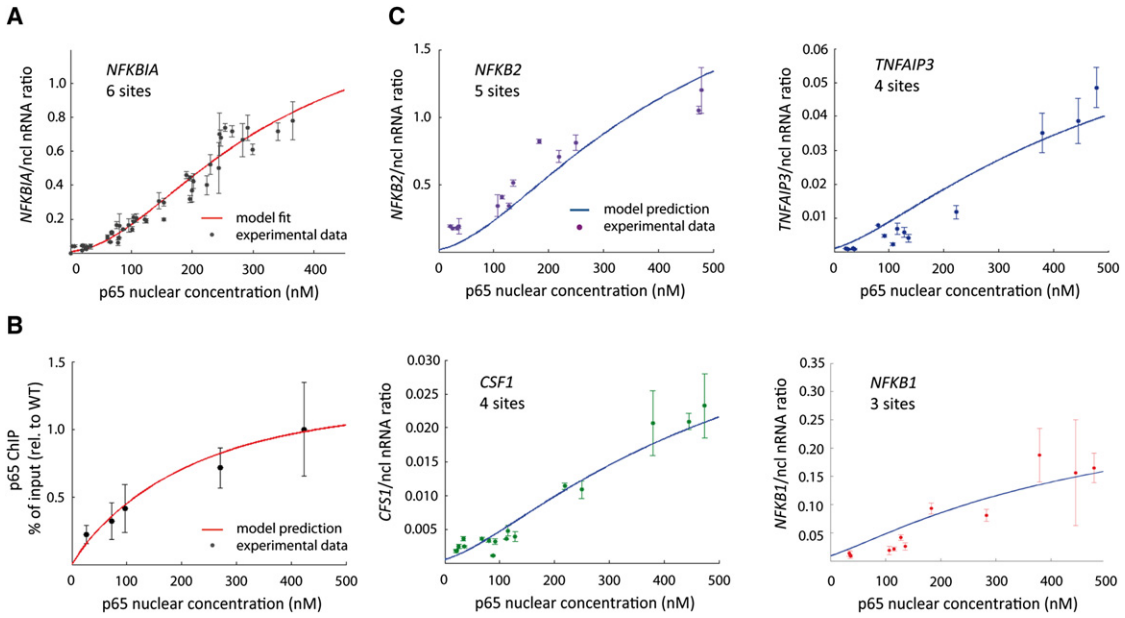

Figure 4. κB Sites in a Cluster Are Used in an Additive Fashion to Recruit Pol II and Initiate Transcription

(A) Best model fit to *NFKBIA* transcriptional induction. The data collected in HCT 116 cells treated with increasing doses of TNF-α (two independent experiments, Figure 2C) and in HCT 116 p65 knockdown clones (six independent experiments, Figure 2E) were merged, and model variant 3 (see Figure 3C) was fitted to the data. In this model, Pol II is attracted in an additive fashion by NF-κB bound to the six sites in the *NFKBIA* promoter. The red curve is representative of any of the fits obtained by imposing a value between 20 and 300 nM for the NF-κB binding affinity to specific sites.

(B) Average p65 recruitment to the six NF-κB binding sites in the *NFKBIA* promoter as a function of p65 nuclear concentration. Anti-p65 ChIP was performed in different p65 knockdown clones stimulated with 10 ng/ml TNF-α for 20 min, and immunoprecipitated DNA was amplified by Q-PCR with *NFKBIA* promoter-specific primers. Mean values ± Q-PCR error propagated from SD of technical replicates of a single representative experiment are plotted. Red line, the prediction of model variant 3 for p65 recruitment on a cluster of six sites. Parameters were chosen among those allowing a good fit of *NFKBIA* induction (see A) in order to return the best agreement with the ChIP data. The NF-κB binding constant is 200 nM, and the NF-κB binding to DNA is noncooperative.

(C) The parameter set determined in (B) was used to predict the shape of the transcriptional induction profiles of genes with different numbers of sites (see Table 1), and rescaled by a multiplicative factor in order to be compared to the experimental data. Mean values ± Q-PCR error propagated from SD of technical replicates of a single experiment are plotted. The *NFKB2* induction profile was predicted imposing five κB sites (cluster 1 in Table 1, corresponding to the shorter annotated transcript, NM_002502). The predicted induction with four κB sites (representing the case where cluster 2 controls the transcriptional induction) is shown in Figure S8.

scheme 3). Cooperativity in TF binding to adjacent sites within the cluster can be introduced into any of these three schemes, independently of the hypothesis on site usage in Pol II recruitment. The different qualitative behavior of the transcriptional induction profiles predicted by the three variants of the model arises from the presence of more than one κB site (Figure S2).

We compared the predictions of the model resulting from each of these three hypotheses with the experimental data on the induction profile of *NFKBIA* and the other NF-κB target genes. All three models returned acceptable fits of the *NFKBIA* induction profile, indicating that they can be parameterized to fit each other. However, the regions of the parameter space that give equivalent fits are well separated and return qualitatively different predictions that can be distinguished experimentally (see below and Figure S3). To evaluate the agreement of the model predictions with the data, we used an approach relying on the estimation of the Bayesian probability that a specific hypothesis will return the observed experimental data (see the Supplemental Information). The hypothesis most compatible with the experimental observations was that every site in the cluster, once bound by NF-κB, recruits Pol II additively (Figure 3C, scheme 3). The *NFKBIA* induction profile could be fitted accurately with this model by imposing that (1) the promoter contains six κB sites, irrespective of their evolutionary constraint (five sites are conserved and one is nonconserved; see Table 1); this choice is motivated by the assumption that all high-affinity sites are functional, even if not conserved; and (2) the equilibrium constant for NF-κB binding to κB sites in the cluster is between 20 and 300 nM, corresponding to the range of affinities observed in vitro for single κB sites (Figure 4A) (Fusco et al., 2009; Phelps et al., 2000).

However, fitting the data with different binding affinities resulted in different estimates of NF-κB binding cooperativity to adjacent sites (see the Supplemental Information). To directly determine if NF-κB binding is cooperative or not, we measured by ChIP the average recruitment of NF-κB to the cluster of binding sites in the *NFKBIA* promoter as a function of NF-κB concentration in p65 knockdown clones stimulated with TNF (Figure 4B). We then asked the model to predict the profile of NF-κB recruitment to the cluster for every set of parameters extracted by the fit to the *NFKBIA* transcriptional profile. The best agreement between the experimental data and the model

prediction was found in the case where NF-κB binding to DNA is noncooperative and the binding constant is 200 nM (Supplemental Information).

It should be stressed that even when only the five conserved κB sites in the *NFKBIA* promoter are considered in the analysis, the hypothesis that best recapitulates the experimental observations remains the same, namely that Pol II is additively recruited by multiple NF-κB molecules bound to the cluster and that binding cooperativity is not required to reproduce the induction profiles. The only remarkable difference when performing the analysis with 5 κB sites is that the optimal agreement with the experimental data occurs at a lower value of the NF-κB binding constant (150 nM, see the Supplemental Information).

To confirm the validity of our noncooperativity interpretation, we asked the model to predict the induction profiles of four other NF-κB target genes: *TNFAIP3*, *NFKB2*, *NFKB1*, and *CSF1*, whose promoter regions contain five (*NFKB2*), four (*CSF1* and *TNFAIP3*), and three (*NFKB1*) κB sites (Table 1). With the exception of *CSF1*, all these genes are components of the NF-κB pathway. Therefore, we assume that their induction is mainly dependent on NF-κB, with marginal contribution by other TFs. Using the parameters extracted from the *NFKBIA* analysis (notably the absence of cooperativity in NF-κB binding), we found excellent agreement between the predicted transcriptional activation profiles of these four genes and the experimental data obtained in p65 knockdown clones (Figure 4C). Therefore, our model provides an accurate description of the transcriptional activity of genes regulated by clustered κB sites.

To further validate our modeling strategy, and specifically to verify its ability to detect cooperativity, we analyzed a transcriptional response involving a cooperative TF, namely Bcd-dependent regulation of Hunchback (Hb) in *D. melanogaster* (see Figure S4 and the discussion thereafter). We found that both models 1 and 3 could fit the Hb induction profile as a function of Bcd nuclear concentration (retrieved from the FlyEx database) (Pisarev et al., 2009) in the whole range of in vitro-measured Bcd affinities (Figures S4C and S4D). The fit returned strong binding cooperativity in a significant range of Bcd binding affinities (Figures S4E and S4F), demonstrating that our model can detect binding cooperativity and coherently describe the output of a cooperative system.

DISCUSSION

The well-established model of transcriptional regulation of developmental genes implies that genes exist in just two alternative functional states, active and inactive. In this context, intermediate levels of activation occur only in the transition between these two states and are confined to narrow regimes of TF concentration in order to be also confined spatially and/or temporally during developmental processes (Gregor et al., 2007). Conversely, environmental genes like inflammatory genes may need to be expressed in a continuum of activation states, each being physiologically relevant in reflecting the intensity of the inflammatory stimulus.

In this study we combined quantitative measurements and thermodynamic modeling to investigate the transcriptional i/o relationship occurring at NF-κB-regulated genes induced by a canonical inflammatory stimulus. Contrary to the expectation that homotypic clusters of high-affinity κB sites would generate cooperativity, we observed an analog relationship between stimulus intensity, nuclear concentration of TF, and transcriptional output, wherein a gradual increase in TF concentration resulted in gradually increasing transcriptional activity.

We designed a minimal, coarse-grained model that captures the essential mechanisms operating at promoters and which is defined by a very limited number of parameters. We used quantitative information on TF concentrations and transcriptional activities, together with known in vitro values of the NF-κB DNA binding constant, to run the model. Hence, our modeling strategy was strongly grounded on experimental measurements, so that we could fit the data with a minimum number of free parameters that cannot be measured (e.g., the effective forces controlling the attractive interaction of TFs and Pol II, mediated by an undefined number of intermediates). We checked the consistency of the fitted parameter values by challenging the model to predict new experimental data. By combining fitting procedures and ChIP experiments, we were able to infer that *noncooperative* binding of NF-κB to adjacent sites in a cluster is at the origin of the analog behavior of the transcriptional response.

Our findings reveal a novel paradigm in the usage of clustered TF binding sites, which differs radically from the well-accepted understanding of developmental transcriptional regulation. In this latter case, protein-protein interactions between TFs are thought to promote cooperativity in DNA binding. This results in sharp transitions between the nonoccupied, inactive state of the promoter and the fully occupied and active state as the TF concentration increases across the dissociation constant for TF binding to cognate sites. This mechanism, which is essential to establish precisely demarcated boundaries between adjacent body regions during development, relies on structural properties of the TF that enable cooperative binding and that can be defined molecularly, as revealed in a genetic screen of Bcd mutants defective in their ability to cooperate in DNA binding (Lebrecht et al., 2005). Hence, cooperative binding to adjacent DNA sites in CRE depends on specific molecular features of the TF.

p50/p52 dimers have been shown to form mutual interactions when bound to adjacent sites in a viral enhancer, the HIV LTR (Moorthy et al., 2007). This suggests that in specific cases cooperativity may also occur in the NF-κB system. However, the 4 bp distance between sites in the HIV LTR is not optimal for promoting maximal interactions between adjacently bound dimers, which occurs at smaller (2 bp) site-to-site distances; notably, this distance is much smaller than the average intersite distance in the 23 promoters considered in our study (Table 1). An intriguing possibility is that evolution has selected site-to-site distances that exclude cooperative NF-κB binding to DNA but that allow multiple interactions of the bound TFs with the transcription preinitiation complex. In other words, at inflammatory genes (and possibly other environmental response genes) lack of cooperative interactions may be hardwired in the genome by the organization of clustered binding sites in CREs. By using our model in the identified regime of *NFKBIA* promoter operation, we simulated what would happen if κB sites in the *NFKBIA* promoter were brought closer, by artificially increasing the cooperative

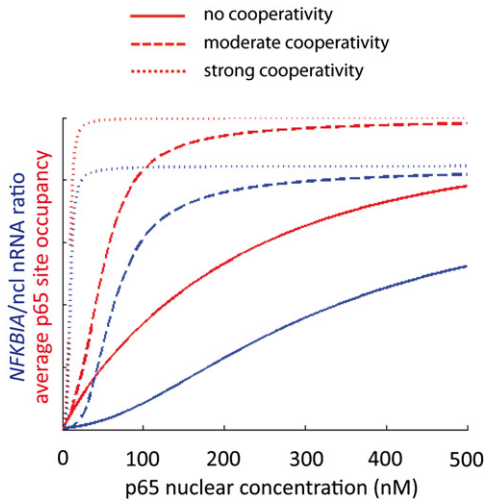

Figure 5. Simulating the Effect of NF-κB Binding Cooperativity

The *NFKBIA* transcriptional activity (blue) and NF-κB recruitment on the promoter cluster (red) upon the experimentally determined conditions (NF-κB binding constant 200 nM, no binding cooperativity, solid lines), and in the simulated presence of mild (dashed lines) and strong (dotted lines) NF-κB binding cooperativity. The Hill coefficients of the NF-κB recruitment profiles (red lines) are 1.1, 2.2, and 4.5, respectively.

binding energy parameter and leaving all other parameters unchanged (Figure 5). Increasing the degree of binding cooperativity completely disrupts the gradual i/o relationship, giving rise to more and more "digital" responses in which the system reacts abruptly to progressive increases in the stimulus. Even when the NF-κB recruitment profile on the cluster is moderately sigmoidal as a consequence of mild binding cooperativity (dashed red line in Figure 5), the predicted transcriptional response is unable to reproduce the experimental data.

What is the regulatory logic that employs clusters with different numbers of sites that do not promote TF binding cooperativity? One possibility is that the number of sites modulates the sensitivity of the transcriptional response to changes in NF-κB nuclear concentration (Figure S5A). Genes with a high number of κB sites would have much higher sensitivity to changes in NF-κB nuclear concentration as compared to genes with fewer sites. Thus, *NFKBIA* (six sites) should be 160 times more sensitive than a gene with just one site, or 12 times more sensitive than a gene with three sites (Figure S5B).

Another (not mutually exclusive) possibility is that the number of sites impacts on the intrinsic noise in transcription arising from fluctuations in the interactions of the transcriptional apparatus with the promoter. This noise is conceptually different from the extrinsic noise arising from cell-to-cell differences in TF concentration (Swain et al., 2002). Using the model in the experimentally determined regime, we calculated the transcriptional intrinsic noise-over-signal ratio (i.e., the spread of the distribution of Pol II occupancy over the population, divided by the average value of Pol II occupancy, given a fixed value of NF-κB concentration) and found that genes with many sites have a much higher intrinsic fidelity as compared to genes with one or a few sites (Figure S5C). Thus, a high number of sites impart robustness, which may be essential to achieve low cell-to-cell variability in *NFKBIA* expression and timing of NF-κB oscillations (Ashall et al., 2009; Hoffmann et al., 2002). Conversely, robustness may not be essential for genes encoding secreted factors, whose promoters have a lower number of sites, because the effects of high noise at the single-cell level would be smoothened when averaged over a large population of cells in a tissue. Experimental observations (Weinmann et al., 2001) support the existence of intrinsically high levels of noise in cytokine gene expression.

From a biological point of view, the needs of an environmental response are in general different from those of a developmental program. In order to prevent over- or underreactions, responses to environmental changes must reflect the strength of the stimulus. Therefore, quantitative information on signal strength must be retained during signal transduction, and gene activation mechanisms must enable the maintenance of gradual i/o relationships. In the case of inflammation, the usage of on/off transcriptional responses is predicted to generate either a suboptimal reaction or no reaction at all if the activation threshold (e.g., microbial load) is not reached, or conversely an excessive and potentially pathogenic inflammatory response if the stimulus exceeds the threshold. Conversely, analog transcriptional responses may be incompatible with the generation of body patterns, leading to poorly defined anatomical borders. We suggest that cooperative and noncooperative TF binding and gene activation reflect alternative strategies selected by evolution for different biological processes. Noncooperative interactions of TFs with their cognate sites may be a common phenomenon encoded in the genome to enable a broad dynamic range of cellular responses to varying strengths of environmental challenges.

EXPERIMENTAL PROCEDURES

Genome Scanning

The proximal promoters of 24,398 human RefSeq genes were scanned for matches to the NF-κB PWM (Grilli et al., 1993). Proximal promoters were defined as 1000 bp upstream to 200 bp downstream of the annotated TSS; all RefSeq annotated exons were masked. The hg18 version of the human genome was downloaded from the UCSC genome repository. κB sites were defined as a match to the PWM scoring above 8.0. Conservation was determined by counting the number of κB sites identified at aligned positions in any of the 11 mammalian genomes: chimpanzee, macaque, mouse, rat, rabbit, cow, dog, armadillo, elephant, tenrec, and opossum. Clusters were defined as sets of κB sites within 400 bp of each other.

Cell Lines

Human colorectal carcinoma HCT116 cells were cultured in McCoy's 5A Glutamax medium supplemented with 10% fetal calf serum. Stable p65 knockdown clonal cell lines were obtained by FuGENE transfection of HCT116 cells with the LMP vector driving the expression of a custom hairpin (5′-CCCG GATTGAGGAGAAACGTAA-3′) directed against nucleotides 1019–1040 of the *RELA* transcript. p65 levels in puromycin-selected clones were assessed by western blot.

Antibodies and Reagents

Anti-p65 (SC-372) and anti-Pol II (SC-899) were from Santa Cruz Biotechnology. Human recombinant TNF-α (R&D Systems) was used at the indicated concentrations (from 0.04 to 10 ng/ml).

Analysis of Nascent Transcripts

Chromatin-associated transcripts were isolated as described (Masternak et al., 2003) with minor modifications (Supplemental Experimental Procedures). Primer sequences are in Table S1. Primers were tested for linearity within at least 3 logs of cDNA concentration.

Nuclear Extracts

Cells (6×10^6) were counted in triplicate, washed three times in ice-cold PBS, and lysed in 300 μl of lysis buffer (50 mM Tris [pH 8.0], 2 mM EDTA [pH 8.0], 0.1% NP-40, 10% glycerol, 1 mM DTT, supplemented with protease inhibitors). After pelleting, nuclei were washed in 300 μl of lysis buffer, resuspended in 50 μl AM1 lysis buffer (Active Motif), and lysed for 30 min on ice. Insoluble nuclear fractions were pelleted at 13,000 rpm for 10 min in a microfuge. Greater than 90% of nuclear p65 remained in the soluble fraction of the nuclear extract (Figure S6).

Quantification of p65 Nuclear Concentration

Three microliters of the soluble nuclear fractions (3/50th of the total number of cells) were loaded in duplicate on a Trans-AM NF-κB colorimetric ELISA plate (Active Motif). Unbound p65 in the postreaction supernatant was detected by western blot (Figure S7). The p65 content of each well was quantified according to manufacturer's instructions, using recombinant p65 as a standard. We obtained the average number of p65 molecules per cell by dividing the number of p65 molecules by the number of cells loaded in a single well. We acquired confocal stacks of the DAPI-stained nuclei of N = 100 cells and extracted the average nuclear volume with the Object Counter 3D ImageJ plugin (see the Supplemental Information). We obtained the average p65 nuclear concentration by dividing the average number of p65 molecules per cell by the average nuclear volume.

Chromatin Immunoprecipitation

ChIP experiments were performed as described previously (Bosisio et al., 2006). Primer sequences are provided in Table S1.

Physical Model of Promoter Operation

Please refer to the Supplemental Information.

Data Fitting

All data analysis and fitting were performed using custom Mathematica routines. Please refer to the Supplemental Information, section titled "Analysis and fitting of transcriptional induction profiles."

SUPPLEMENTAL INFORMATION

Supplemental Information includes eight figures, one table, Supplemental Experimental Procedures, Analysis and Fitting of Transcriptional Induction Profiles, and Thermodynamic Model of NF-κB-Dependent Promoter Operation and can be found with this article online at doi:10.1016/j.molcel.2010.01.016.

ACKNOWLEDGMENTS

We thank A. Ciliberto for comments on the manuscript. This work was funded by the Human Frontier Science Program (HFSP) (Young Investigator Grant #RGY0085/2005-C to M.P., G.N., and M.L.B.); by the European Commission (EC) (FP6 Marie Curie Excellence Grant TRANS-TAR, and FP7 "Model-In" grant to G.N.); and by the AIRC (Italian Association for Research on Cancer). L.G. was supported by a fellowship from the Italian Institute of Technology (IIT).

Received: August 5, 2009
Revised: October 30, 2009
Accepted: December 23, 2009
Published: February 11, 2010

REFERENCES

Arnone, M.I., and Davidson, E.H. (1997). The hardwiring of development: organization and function of genomic regulatory systems. Development *124*, 1851–1864.

Ashall, L., Horton, C.A., Nelson, D.E., Paszek, P., Harper, C.V., Sillitoe, K., Ryan, S., Spiller, D.G., Unitt, J.F., Broomhead, D.S., et al. (2009). Pulsatile stimulation determines timing and specificity of NF-kappaB-dependent transcription. Science *324*, 242–246.

Berman, B.P., Nibu, Y., Pfeiffer, B.D., Tomancak, P., Celniker, S.E., Levine, M., Rubin, G.M., and Eisen, M.B. (2002). Exploiting transcription factor binding site clustering to identify cis-regulatory modules involved in pattern formation in the Drosophila genome. Proc. Natl. Acad. Sci. USA *99*, 757–762.

Bintu, L., Buchler, N.E., Garcia, H.G., Gerland, U., Hwa, T., Kondev, J., and Phillips, R. (2005). Transcriptional regulation by the numbers: models. Curr. Opin. Genet. Dev. *15*, 116–124.

Birney, E., Stamatoyannopoulos, J.A., Dutta, A., Guigo, R., Gingeras, T.R., Margulies, E.H., Weng, Z., Snyder, M., Dermitzakis, E.T., Thurman, R.E., et al. (2007). Identification and analysis of functional elements in 1% of the human genome by the ENCODE pilot project. Nature *447*, 799–816.

Bosisio, D., Marazzi, I., Agresti, A., Shimizu, N., Bianchi, M.E., and Natoli, G. (2006). A hyper-dynamic equilibrium between promoter-bound and nucleoplasmic dimers controls NF-kappaB-dependent gene activity. EMBO J. *25*, 798–810.

Burz, D.S., Rivera-Pomar, R., Jackle, H., and Hanes, S.D. (1998). Cooperative DNA-binding by Bicoid provides a mechanism for threshold-dependent gene activation in the Drosophila embryo. EMBO J. *17*, 5998–6009.

Darzacq, X., Shav-Tal, Y., de Turris, V., Brody, Y., Shenoy, S.M., Phair, R.D., and Singer, R.H. (2007). In vivo dynamics of RNA polymerase II transcription. Nat. Struct. Mol. Biol. *14*, 796–806.

Fusco, A.J., Huang, D.B., Miller, D., Wang, V.Y., Vu, D., and Ghosh, G. (2009). NF-kappaB p52:RelB heterodimer recognizes two classes of kappaB sites with two distinct modes. EMBO Rep. *10*, 152–159.

Gonzalez-Crespo, S., and Levine, M. (1993). Interactions between dorsal and helix-loop-helix proteins initiate the differentiation of the embryonic mesoderm and neuroectoderm in Drosophila. Genes Dev. *7*, 1703–1713.

Gregor, T., Tank, D.W., Wieschaus, E.F., and Bialek, W. (2007). Probing the limits to positional information. Cell *130*, 153–164.

Grilli, M., Chiu, J.J., and Lenardo, M.J. (1993). NF-kappa B and Rel: participants in a multiform transcriptional regulatory system. Int. Rev. Cytol. *143*, 1–62.

Gumucio, D.L. (1991). γ-globin gene regulation: evolutionary approaches. In The Regulation of Hemoglobin Switching. Proceedings of the Seventh Conference on Hemoglobin Switching, G. Stamatoyannopoulos and A.W. Nienhuis, eds., pp. 277–289.

Hayden, M.S., and Ghosh, S. (2008). Shared principles in NF-kappaB signaling. Cell *132*, 344–362.

Hoffmann, A., Levchenko, A., Scott, M.L., and Baltimore, D. (2002). The IkappaB-NF-kappaB signaling module: temporal control and selective gene activation. Science *298*, 1241–1245.

Hoffmann, A., Leung, T.H., and Baltimore, D. (2003). Genetic analysis of NF-kappaB/Rel transcription factors defines functional specificities. EMBO J. *22*, 5530–5539.

Huang, K. (1987). Statistical Mechanics (New York: Wiley).

Ip, Y.T., Park, R.E., Kosman, D., Yazdanbakhsh, K., and Levine, M. (1992). dorsal-twist interactions establish snail expression in the presumptive mesoderm of the Drosophila embryo. Genes Dev. *6*, 1518–1530.

Ishii, H. (2000). A statistical-mechanical model for regulation of long-range chromatin structure and gene expression. J. Theor. Biol. *203*, 215–228.

Lahav, G., Rosenfeld, N., Sigal, A., Geva-Zatorsky, N., Levine, A.J., Elowitz, M.B., and Alon, U. (2004). Dynamics of the p53-Mdm2 feedback loop in individual cells. Nat. Genet. *36*, 147–150.

Lebrecht, D., Foehr, M., Smith, E., Lopes, F.J., Vanario-Alonso, C.E., Reinitz, J., Burz, D.S., and Hanes, S.D. (2005). Bicoid cooperative DNA binding is critical for embryonic patterning in Drosophila. Proc. Natl. Acad. Sci. USA *102*, 13176–13181.

Lifanov, A.P., Makeev, V.J., Nazina, A.G., and Papatsenko, D.A. (2003). Homotypic regulatory clusters in Drosophila. Genome Res. *13*, 579–588.

Markstein, M., Markstein, P., Markstein, V., and Levine, M.S. (2002). Genome-wide analysis of clustered Dorsal binding sites identifies putative target genes in the Drosophila embryo. Proc. Natl. Acad. Sci. USA *99*, 763–768.

Masternak, K., Peyraud, N., Krawczyk, M., Barras, E., and Reith, W. (2003). Chromatin remodeling and extragenic transcription at the MHC class II locus control region. Nat. Immunol. *4*, 132–137.

Maury, C.P. (1989). Monitoring the acute phase response: comparison of tumour necrosis factor (cachectin) and C-reactive protein responses in inflammatory and infectious diseases. J. Clin. Pathol. *42*, 1078–1082.

Moorthy, A.K., Huang, D.B., Wang, V.Y., Vu, D., and Ghosh, G. (2007). X-ray structure of a NF-kappaB p50/RelB/DNA complex reveals assembly of multiple dimers on tandem kappaB sites. J. Mol. Biol. *373*, 723–734.

Munoz, V. (2001). What can we learn about protein folding from Ising-like models? Curr. Opin. Struct. Biol. *11*, 212–216.

Natoli, G., Saccani, S., Bosisio, D., and Marazzi, I. (2005). Interactions of NF-kappaB with chromatin: the art of being at the right place at the right time. Nat. Immunol. *6*, 439–445.

Palmeri, J., Manghi, M., and Destainville, N. (2008). Thermal denaturation of fluctuating finite DNA chains: the role of bending rigidity in bubble nucleation. Phys. Rev. E Stat. Nonlin. Soft Matter Phys. *77*, 011913.

Phelps, C.B., Sengchanthalangsy, L.L., Malek, S., and Ghosh, G. (2000). Mechanism of kappa B DNA binding by Rel/NF-kappa B dimers. J. Biol. Chem. *275*, 24392–24399.

Pisarev, A., Poustelnikova, E., Samsonova, M., and Reinitz, J. (2009). FlyEx, the quantitative atlas on segmentation gene expression at cellular resolution. Nucleic Acids Res. *37*, D560–D566.

Podtschaske, M., Benary, U., Zwinger, S., Hofer, T., Radbruch, A., and Baumgrass, R. (2007). Digital NFATc2 activation per cell transforms graded T cell receptor activation into an all-or-none IL-2 expression. PLoS ONE *2*, e935. 10.1371/journal.pone.0000935.

Ponting, C.P. (2008). The functional repertoires of metazoan genomes. Nat. Rev. Genet. *9*, 689–698.

Roth, S., Stein, D., and Nusslein-Volhard, C. (1989). A gradient of nuclear localization of the dorsal protein determines dorsoventral pattern in the Drosophila embryo. Cell *59*, 1189–1202.

Segal, E., Raveh-Sadka, T., Schroeder, M., Unnerstall, U., and Gaul, U. (2008). Predicting expression patterns from regulatory sequence in Drosophila segmentation. Nature *451*, 535–540.

Stathopoulos, A., and Levine, M. (2002). Linear signaling in the Toll-Dorsal pathway of Drosophila: activated Pelle kinase specifies all threshold outputs of gene expression while the bHLH protein Twist specifies a subset. Development *129*, 3411–3419.

Stein, D., Goltz, J.S., Jurcsak, J., and Stevens, L. (1998). The Dorsal-related immunity factor (Dif) can define the dorsal-ventral axis of polarity in the Drosophila embryo. Development *125*, 2159–2169.

Swain, P.S., Elowitz, M.B., and Siggia, E.D. (2002). Intrinsic and extrinsic contributions to stochasticity in gene expression. Proc. Natl. Acad. Sci. USA *99*, 12795–12800.

Tetta, C., Camussi, G., Modena, V., Di Vittorio, C., and Baglioni, C. (1990). Tumour necrosis factor in serum and synovial fluid of patients with active and severe rheumatoid arthritis. Ann. Rheum. Dis. *49*, 665–667.

Walters, M.C., Fiering, S., Eidemiller, J., Magis, W., Groudine, M., and Martin, D.I. (1995). Enhancers increase the probability but not the level of gene expression. Proc. Natl. Acad. Sci. USA *92*, 7125–7129.

Weinmann, A.S., Mitchell, D.M., Sanjabi, S., Bradley, M.N., Hoffmann, A., Liou, H.C., and Smale, S.T. (2001). Nucleosome remodeling at the IL-12 p40 promoter is a TLR-dependent, Rel-independent event. Nat. Immunol. *2*, 51–57.

Werner, S.L., Kearns, J.D., Zadorozhnaya, V., Lynch, C., O'Dea, E., Boldin, M.P., Ma, A., Baltimore, D., and Hoffmann, A. (2008). Encoding NF-kappaB temporal control in response to TNF: distinct roles for the negative regulators IkappaBalpha and A20. Genes Dev. *22*, 2093–2101.